ERDC/GSL TR-12-13

Geotechnical and Structures Laboratory

US Army Corps
of Engineers®
Engineer Research and
Development Center

Structure-Property Relationships of Steel Cylindrical Shells

Ruth G. Hidalgo-Hernandez, Paul G. Allison,
Brett A. Williams, Luis A. de Béjar, W. Scott Hart,
and Jason Morson

March 2012

ERDC/GSL TR-12-13
March 2012

Structure-Property Relationships of Steel Cylindrical Shells

Ruth G. Hidalgo-Hernandez, Paul G. Allison, Brett A. Williams, Luis A. de Béjar, W. Scott Hart, and Jason Morson

Geotechnical and Structures Laboratory
U.S. Army Engineer Research and Development Center
3909 Halls Ferry Road
Vicksburg, MS 39180-6199

Final report

Prepared for U.S. Army Corps of Engineers
Washington, DC 20314-1000

Abstract

Personnel of the U.S. Army Engineer Research and Development Center (ERDC), Geotechnical and Structures Laboratory (GSL), Engineering Systems and Materials Division (ESMD), Concrete and Materials Branch (CMB), Vicksburg, Mississippi, were asked to examine the mechanical properties and microstructure characteristics of a commercially available steel cylindrical shell in its as-manufactured condition. To examine the mechanical properties, uniaxial tensile experiments were performed on ASTM dog-bone specimens and hoop cross-sectional specimens at displacement rates of 0.1 in./min., to obtain the stress-strain material responses. A commercially available image-analysis program determined the void volume fraction (VVF), the nearest neighbor distance (NND) of pores, maximum and minimum pore sizes, and aspect ratio of the pores at 30-degree increments of the steel hoop cross-sections. The results of the investigation allow for an improved understanding of the mechanical behavior of steel cylindrical shells.

Contents

Figures and Tables

Figures

Tables

Preface

This study of steel cylindrical shells was conducted in 2011 by personnel of the U.S. Army Engineer Research and Development Center (ERDC), Geotechnical and Structures Laboratory (GSL), Vicksburg, Mississippi. It was funded through the Military Engineering Basic Research Program, Work Unit AR031, "Geo-statistical characterization of micro-structural defects and statistical physics modeling of shell-case fragmentation in ammunition steel cases." The Work Unit Principal Investigator was Dr. Luis A. de Béjar of the GSL's Structural Mechanics Branch (SMB).

The research was conducted by the GSL's Engineering Systems and Materials Division (ESMD), Concrete and Materials Branch (CMB). Laboratory characterization tests and analyses of the results were performed by Ruth G. Hidalgo-Hernandez, Dr. Paul A. Allison, Brett A. Williams, W. Scott Hart, and Jason Morson, all of the CMB. Hidalgo-Hernandez and Allison prepared this report.

During the investigation, Christopher M. Moore was Acting Chief, CMB; Dr. Larry N. Lynch was Chief, ESMD; Dr. William P. Grogan was Deputy Director, GSL; and Dr. David W. Pittman was Director, GSL.

COL Kevin J. Wilson was Commander and Executive Director of ERDC. Dr. Jeffery P. Holland was Director.

Unit Conversion Factors

Multiply	By	To Obtain
degrees (angle)	0.01745329	radians
feet	0.3048	meters
foot-pounds force	1.355818	joules
inches	0.0254	meters
inch-pounds (force)	0.1129848	newton meters
microns	1.0 E-06	meters
pounds (force)	4.448222	newtons
pounds (force) per foot	14.59390	newtons per meter
pounds (force) per inch	175.1268	newtons per meter
pounds (force) per square foot	47.88026	pascals
pounds (force) per square inch	6.894757	kilopascals

1 Introduction

Background

Personnel of the U.S. Army Engineer Research and Development Center (ERDC), Geotechnical and Structures Laboratory (GSL), conducted a series of laboratory experiments to measure the mechanical properties and evaluate the microstructure characteristics of a commercially available steel pipe in its as-manufactured condition. The mechanical property tests consisted of uniaxial tensile experiments performed on dog-bone specimens and hoop cross-sectional specimens at a constant displacement rate. In addition, a commercially available image-analysis program was used to determine the microstructural features such as void volume fraction, maximum and minimum pore size, the distance to the pores' nearest neighbors, and aspect ratio of the pores at 30-degree increments of the steel hoop cross-sections.

Purpose and scope

The purpose of this project was to obtain baseline experimental data on mechanical behavior and microstructure of the steel cylindrical shells. The collected data will be used for the assessment of geo-statistical techniques that simulate cross-sectional porosity for mechanical analyses of crack initiation, growth, propagation, and coalescence when subjected to impulsive internal loads.

Chapter 2 provides a description of the experimental procedures, and experimental results are in Chapter 3. A summary of the investigation is in Chapter 4.

2 Experimental Procedure

Monotonic tensile experiments

An MTS 110-kip load frame was used to conduct three monotonic tensile experiments on a low-carbon-alloy steel pipe. Experiments were performed on uniaxial dog-bone-shaped tensile specimens in the longitudinal orientation of the pipe and hoop tensile specimens in the pipe's transverse orientation. The ERDC machine shop prepared the test specimens using a water-jet cutting system.

For the uniaxial monotonic tensile experiments, the load frame monitored force, while an MTS 634.12E-24 extensometer with a 1-in. gage length provided strain data. The experiments were executed at a displacement control rate of 0.1 in./min.

During hoop tensile testing, the load frame monitored force and displacement. Strain data were not available. The hoop tests also were performed in displacement control at a rate of 0.1 in./min. The experimental setup is shown in Figure 1.

Figure 1. Hoop tensile test setup.

Image analysis

Specimen polishing

Sectioned hoop specimens were hand-polished on an Allied High Tech MultiPrep polishing system. The specimens were polished to a surface deviation of +/- 1 μm using the procedure outlined in Table 1. Between each polishing step, sonication using distilled water cleaned the specimens.

Table 1. Details of polishing procedure.

	Abrasive	Lubricant	Time (min)
Step 1	60-grit silicon carbide	distilled water	until plane
Step 2	120-grit silicon carbide	distilled water	3:00
Step 3	240-grit silicon carbide	distilled water	3:00
Step 4	400-grit silicon carbide	distilled water	3:00
Step 5	600-grit silicon carbide	distilled water	3:00
Step 6	800-grit silicon carbide	distilled water	3:00
Step 7	1200-grit silicon carbide	distilled water	3:00
Step 8	1 μm diamond paste	diamond extender	3:00

Optical imaging analysis

A Zeiss Z9Imager captured darkfield images of the polished hoop cross-sections at 30-degree increments. Images were obtained at three locations for each increment around the hoop specimen, as illustrated in Figure 2. The first image was recorded halfway between the inner edge of the specimen and the midpoint. The second image was captured at the midpoint of the specimen, and the third image was obtained halfway between the midpoint and the outer edge of the specimen. A typical image is shown in Figure 3.

An image-analysis software program developed by the Center for Advanced Vehicular Systems at Mississippi State University (MSU-CAVS) calculated void volume fraction (VVF), nearest neighbor distance (NND), pore aspect ratio, and maximum and minimum pore size from each image. T.Y. Stone and others detail the image-analysis procedure used for specimens in the research in their 2009 article in the Journal of Powder Metallurgy.

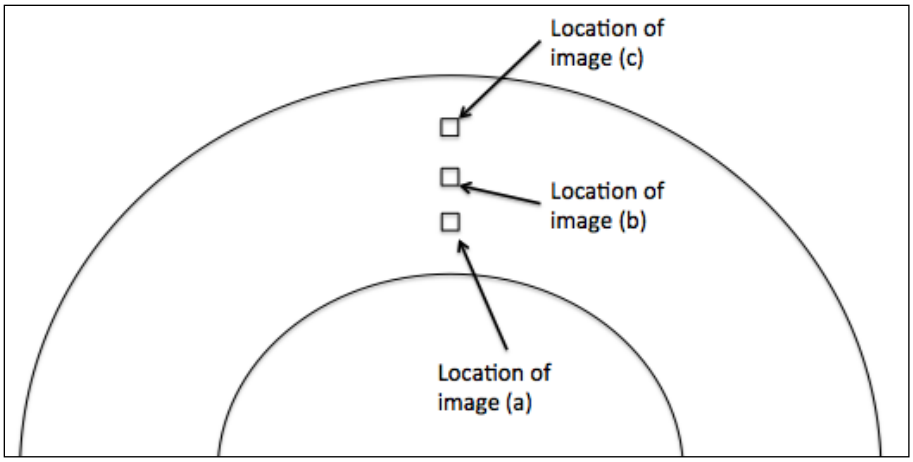

Figure 2. Illustration of the locations of images on hoop cross-sections.

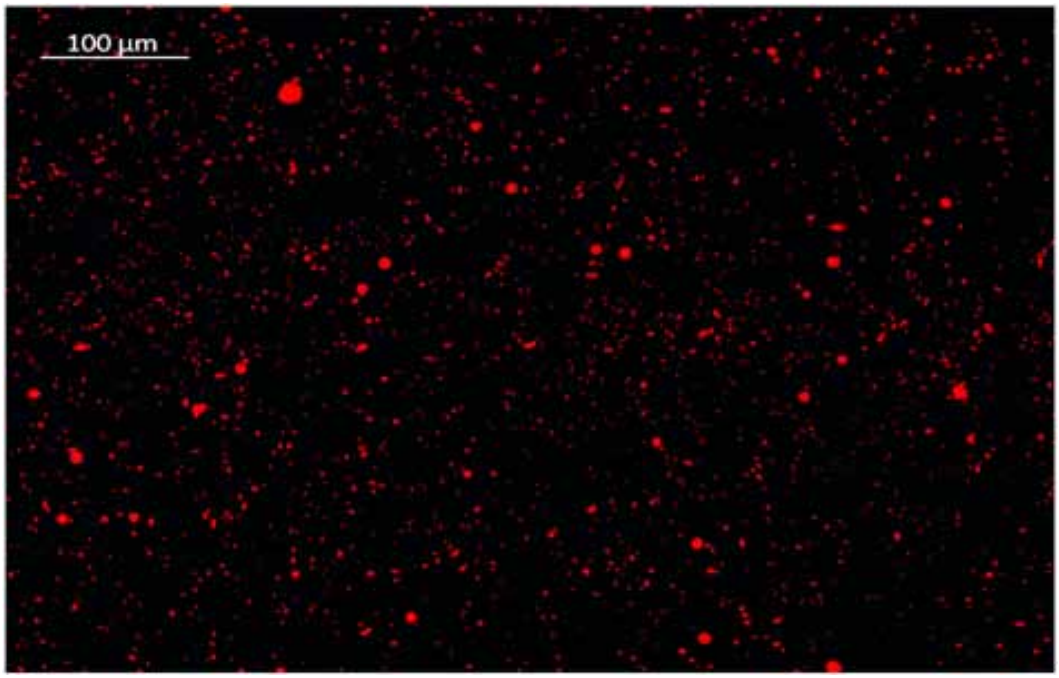

Figure 3. Porosity optical micrographs of Specimen 1 at 0-degree location A.

3 Experimental Results

Tensile experiments

The results of the uniaxial dog-bone tensile experiments are in Figure 4.

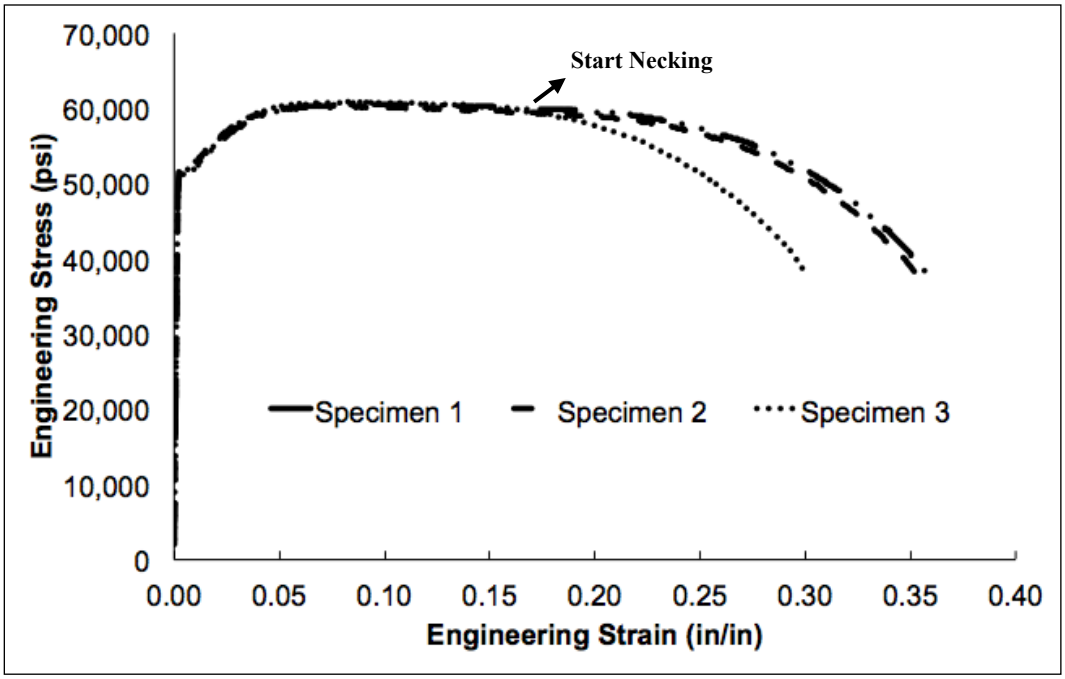

Figure 4. Engineering stress versus strain data for the uniaxial dog-bone experiments.

All three specimens in Figure 4 exhibit similar hardening and recovery in the stress-strain responses. However, the strains to failure for the specimens vary from 0.30 to 0.36 in./in. Young's modulus, ultimate tensile strength, and strain to failure from these experiments are in Table 2.

The force versus displacement relations for the three hoop specimens are in Figure 5.

Table 2. Mechanical properties of monotonic uniaxial dog-bone tensile specimens.

	Ultimate Tensile Strength (ksi)	Young's Modulus (ksi)	Strain-to-failure (in/in)	Yield Stress (ksi)
Specimen 1	61.1	27.1	0.36	51.1
Specimen 2	60.4	27.5	0.35	51.1
Specimen 3	61.0	28.3	0.30	51.2

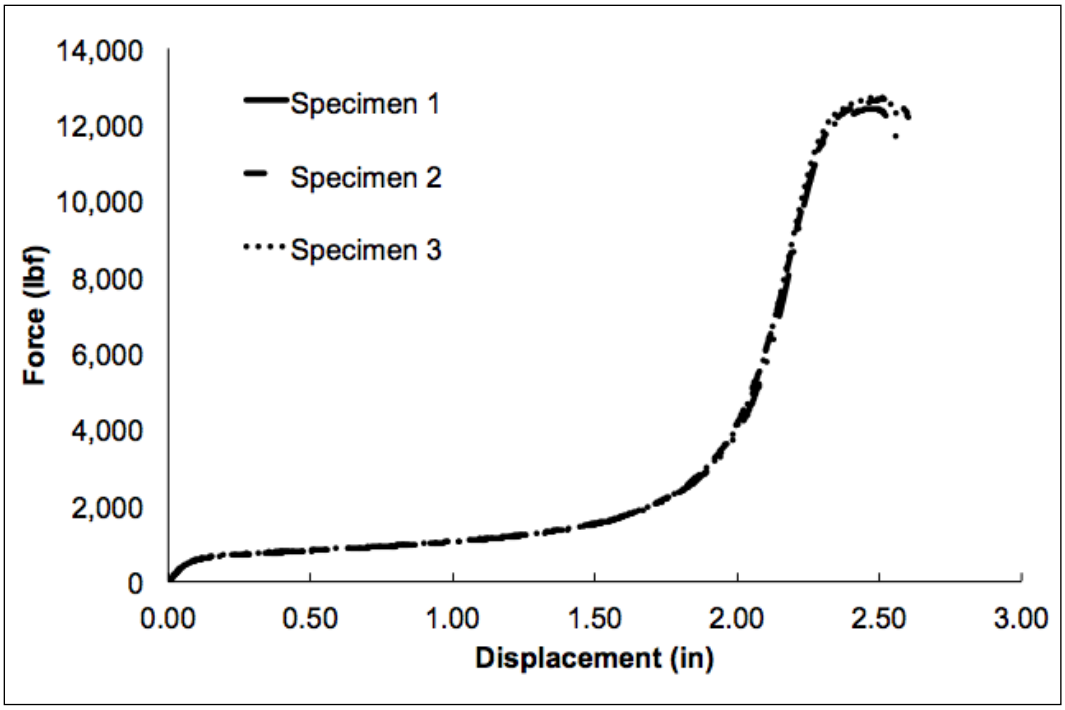

Figure 5. Force versus displacement data for hoop tensile testing.

The data appear similar. The values of maximum force and maximum displacement are in Table 3.

Table 3. Maximum force and displacement values from hoop tensile experiments.

	Maximum Force (lbf)	Maximum Displacement (in)
Specimen 1	12418	2.56003
Specimen 2	12666	2.60156
Specimen 3	12706	2.56348

Image analysis

The image analysis results featuring VVF, maximum and minimum pore size, NND, and aspect ratio of the pores in the hoop cross-sections are in Tables 4 through 12. The images were taken at a magnification of 20X. The minimum pore area that could be resolved at the selected magnification was 1.16 μm.

Table 4. Image analysis results of hoop Specimen 1 (0–90 degrees).

	Void Volume Fraction	Pore Area			Nearest Neighbor Distance			Aspect Ratio		
		Max. (µm)	Min. (µm)	Avg. (µm)	Max. (µm)	Min. (µm)	Avg. (µm)	Max. (µm)	Min. (µm)	Avg. (µm)
0a	0.0282	217	1.16	4.60	25.48	1.84	6.80	4.56	1.00	1.42
0b	0.0437	1408	1.16	6.89	22.11	1.70	6.72	4.24	1.00	1.41
0c	0.0427	4002	1.16	6.73	30.16	1.61	6.83	4.88	1.00	1.39
30a	0.0039	128	1.16	4.87	102.16	1.78	17.64	4.56	1.00	1.45
30b	0.0035	52	1.16	5.53	91.78	1.81	18.95	3.62	1.00	1.44
30c	0.0034	60	1.16	6.51	98.29	2.32	21.84	3.13	1.00	1.39
60a	0.0177	91	1.16	3.98	34.92	1.75	7.72	4.36	1.00	1.54
60b	0.0225	1580	1.16	5.34	43.68	1.31	7.60	4.83	1.00	1.56
60c	0.0080	532	1.16	5.65	67.15	2.36	13.40	4.85	1.00	1.47
90a	0.0120	507	1.16	4.21	41.89	1.62	9.34	3.49	1.00	1.45
90b	0.0120	323	1.16	6.79	39.05	2.03	12.37	3.67	1.00	1.42
90c	0.0101	433	1.16	6.17	50.78	1.72	12.50	5.75	1.00	1.40

Table 5. Image analysis results of hoop Specimen 1 (120–210 degrees).

	Void Volume Fraction	Pore Area			Nearest Neighbor Distance			Aspect Ratio		
		Max. (µm)	Min. (µm)	Avg. (µm)	Max. (µm)	Min. (µm)	Avg. (µm)	Max. (µm)	Min. (µm)	Avg. (µm)
120a	0.0086	116	1.16	4.63	47.63	1.96	12.02	3.49	1.00	1.43
120b	0.0194	1261	1.16	10.10	55.68	1.84	10.29	4.58	1.00	1.49
120c	0.0174	1226	1.16	15.00	58.18	1.86	14.55	4.12	1.00	1.53
150a	0.0151	448	1.16	4.78	27.21	1.64	9.01	5.96	1.00	1.39
150b	0.0096	565	1.16	6.35	53.99	2.27	12.99	4.59	1.00	1.41
150c	0.0143	292	1.16	4.95	30.20	1.87	9.86	3.94	1.00	1.37
180a	0.0153	107	1.16	4.17	32.71	1.87	8.72	3.79	1.00	1.38
180b	0.0157	73	1.16	4.74	45.64	1.80	8.81	4.00	1.00	1.43
180c	0.0230	3310	1.16	13.48	55.66	1.75	10.33	5.54	1.00	1.52
210a	0.0094	588	1.16	5.04	43.17	2.00	11.96	4.77	1.00	1.42
210b	0.0079	177	1.16	4.12	37.64	1.62	11.34	4.02	1.00	1.47
210c	0.0134	475	1.16	4.30	27.19	1.57	8.72	5.25	1.00	1.52

Table 6. Image analysis results of hoop Specimen 1 (240–330 degrees).

	Void Volume Fraction	Pore Area			Nearest Neighbor Distance			Aspect Ratio		
		Max. (µm)	Min. (µm)	Avg. (µm)	Max. (µm)	Min. (µm)	Avg. (µm)	Max. (µm)	Min. (µm)	Avg. (µm)
240a	0.0102	294	1.16	3.86	51.32	1.83	9.71	5.00	1.00	1.48
240b	0.0050	151	1.16	3.29	42.14	2.01	12.41	7.59	1.00	1.51
240c	0.0131	612	1.16	3.66	35.87	1.61	8.17	4.47	1.00	1.46
270a	0.0024	47	1.16	3.90	66.34	1.89	19.61	3.27	1.00	1.42
270b	0.0057	78	1.16	2.87	52.44	1.64	11.04	4.00	1.00	1.46
270c	0.0050	272	1.16	4.24	64.97	1.78	13.56	5.99	1.00	1.47
300a	0.0046	67	1.16	3.66	61.44	2.37	13.29	7.72	1.00	1.48
300b	0.0049	1294	1.16	16.87	78.27	2.49	25.03	3.27	1.00	1.36
300c	0.0039	104	1.16	4.08	98.84	2.01	14.24	3.50	1.00	1.44
330a	0.0042	383	1.16	9.63	69.75	3.29	27.15	3.18	1.00	1.42
330b	0.0035	37	1.16	3.55	47.75	2.04	15.31	4.08	1.00	1.46
330c	0.0032	40	1.16	4.20	64.25	1.71	18.37	3.85	1.00	1.42

Table 7. Image analysis results of hoop Specimen 2 (0–90 degrees).

	Void Volume Fraction	Pore Area			Nearest Neighbor Distance			Aspect Ratio		
		Max. (µm)	Min. (µm)	Avg. (µm)	Max. (µm)	Min. (µm)	Avg. (µm)	Max. (µm)	Min. (µm)	Avg. (µm)
0a	0.0211	621.17	1.16	5.7	31.63	1.57	8.58	6	1	1.58
0b	0.0325	333.56	1.16	7.91	28.95	1.81	7.88	4.12	1	1.6
0c	0.0320	366.52	1.16	8.11	31.95	1.79	7.92	4.45	1	1.58
30a	0.0099	361.02	1.16	6.14	63.41	1.83	11.52	5.05	1	1.53
30b	0.0133	247.14	1.16	7.48	59.7	1.87	10.44	5.05	1	1.62
30c	0.0055	42.78	1.16	4.05	63.87	1.94	11.78	4.47	1	1.58
60a	0.0026	128.92	1.16	3.56	67	1.83	17.23	3.85	1	1.55
60b	0.0060	67.64	1.16	2.47	58.3	1.7	10.03	5	1	1.47
60c	0.0339	244.25	1.15	3.2	24.82	1.53	5.02	5.24	1	1.57
90a	0.0035	44.22	1.16	2.39	52.61	1.94	11.84	3.53	1	1.44
90b	0.0017	41.05	1.16	2.86	93.64	2.03	17.92	3.09	1	1.49
90c	0.0217	239.05	1.16	4.19	39.96	1.48	6.31	5	1	1.64

Table 8. Image analysis results of hoop Specimen 2 (120–210 degrees).

	Void Volume Fraction	Pore Area			Nearest Neighbor Distance			Aspect Ratio		
		Max. (µm)	Min. (µm)	Avg. (µm)	Max. (µm)	Min. (µm)	Avg. (µm)	Max. (µm)	Min. (µm)	Avg. (µm)
120a	0.0204	128.63	1.16	7.88	40.53	2.05	9.12	6.00	1.00	1.67
120b	0.0286	248.58	1.16	7.55	34.95	0.08	7.55	8.15	1.00	1.6
120c	0.0643	559.02	1.16	5.92	31.29	1.149	4.74	6.15	1.00	1.67
150a	0.0134	130	1.16	6.36	49.41	1.79	9.73	7.92	1.00	1.65
150b	0.0083	349	1.16	6.31	54.22	1.86	10.57	6.26	1.00	1.64
150c	0.0145	210	1.16	7.38	38.64	1.64	9.86	7.64	1.00	1.67
180a	0.0355	337	1.16	6.91	29.20	1.63	7.21	5.65	1.00	1.56
180b	0.0299	148	1.16	6.46	28.40	1.61	7.38	5.47	1.00	1.59
180c	0.0245	165	1.16	4.35	28.32	1.57	6.74	10.00	1.00	1.55
210a	0.0194	103	1.16	6.57	36.11	1.61	8.57	5.84	1.00	1.67
210b	0.0372	398	1.16	9.25	28.66	1.61	7.72	7.85	1.00	1.63
210c	0.0300	188	1.16	5.82	28.83	1.88	7.08	7.43	1.00	1.57

Table 9. Image analysis results of hoop Specimen 2 (240–330 degrees).

	Void Volume Fraction	Pore Area			Nearest Neighbor Distance			Aspect Ratio		
		Max. (µm)	Min. (µm)	Avg. (µm)	Max. (µm)	Min. (µm)	Avg. (µm)	Max. (µm)	Min. (µm)	Avg. (µm)
240a	0.0147	82	1.16	3.87	30.96	1.64	8.06	6.18	1.00	1.53
240b	0.0219	251	1.16	4.49	31.72	1.67	7.19	4.55	1.00	1.56
240c	0.0347	563	1.16	3.87	35.17	1.50	5.32	4.80	1.00	1.57
270a	0.0340	439	1.16	4.43	24.58	1.80	6.00	4.00	1.00	1.48
270b	0.0799	344	1.16	6.63	26.43	1.70	5.13	4.98	1.00	1.50
270c	0.0463	296	1.16	7.01	30.23	1.64	6.41	5.73	1.00	1.50
300a	0.0524	1234	1.16	5.05	25.78	1.60	5.37	7.00	1.00	1.51
300b	0.0392	319	1.16	4.17	20.91	1.64	5.51	6.31	1.00	1.46
300c	0.0457	746	1.16	5.27	35.28	1.64	5.88	4.52	1.00	1.47
330a	0.0187	93	1.16	3.28	32.76	1.84	6.83	6.94	1.00	1.48
330b	0.0419	181	1.16	3.98	23.02	1.61	5.36	8.04	1.00	1.53
330c	0.0439	237	1.16	4.98	27.36	1.61	5.66	5.34	1.00	1.50

Table 10. Image analysis results of hoop Specimen 3 (0–90 degrees).

	Void Volume Fraction	Pore Area			Nearest Neighbor Distance			Aspect Ratio		
		Max. (µm)	Min. (µm)	Avg. (µm)	Max. (µm)	Min. (µm)	Avg. (µm)	Max. (µm)	Min. (µm)	Avg. (µm)
0a	0.0036	86.14	1.16	7.51	75.37	3.91	23.77	2.78	1.00	1.33
0b	0.0042	211.59	1.16	8.91	71.07	2.92	24.40	2.86	1.00	1.32
0c	0.0042	82.96	1.16	10.70	77.76	3.64	26.96	2.75	1.00	1.36
30a	0.0045	56.94	1.16	14.48	155.18	2.79	27.49	2.86	1.02	1.40
30b	0.0043	49.14	1.16	7.87	58.30	2.17	21.71	2.86	1.00	1.34
30c	0.0040	68.79	1.16	6.66	66.26	2.38	21.24	5.59	1.00	1.39
60a	0.0046	814.26	1.16	12.61	87.15	2.40	26.26	3.60	1.00	1.34
60b	0.0059	406.41	1.16	12.31	61.78	3.29	21.66	3.68	1.00	1.34
60c	0.0035	60.41	1.16	8.57	75.75	2.68	29.12	3.72	1.00	1.33
90a	0.0039	648.92	1.16	12.03	113.43	5.32	30.07	3.34	1.00	1.35
90b	0.0044	239.91	1.16	11.28	69.53	2.24	26.02	3.91	1.00	1.39
90c	0.0050	269.11	1.16	11.85	76.79	2.65	24.24	4.00	1.00	1.38

Table 11. Image analysis results of hoop Specimen 3 (120–210 degrees).

	Void Volume Fraction	Pore Area			Nearest Neighbor Distance			Aspect Ratio		
		Max. (µm)	Min. (µm)	Avg. (µm)	Max. (µm)	Min. (µm)	Avg. (µm)	Max. (µm)	Min. (µm)	Avg. (µm)
120a	0.0108	1560.59	1.16	24.73	74.90	4.33	23.69	3.34	1.00	1.32
120b	0.0041	101.17	1.16	8.80	88.20	2.62	23.48	3.28	1.00	1.36
120c	0.0034	92.21	1.16	7.03	58.45	2.80	24.19	3.27	1.00	1.32
150a	0.0026	186.73	1.16	10.87	93.18	3.75	32.12	2.75	1.00	1.32
150b	0.0043	75.73	1.16	8.41	98.30	3.08	22.42	9.33	1.00	1.40
150c	0.0053	188.46	1.16	8.62	67.09	2.96	20.15	2.93	1.00	1.34
180a	0.0026	108.11	1.16	9.22	89.88	2.17	29.39	5.00	1.00	1.50
180b	0.0027	104.64	1.16	9.64	89.74	2.55	32.16	4.00	1.00	1.38
180c	0.0040	242.22	1.16	9.31	76.22	3.68	25.09	2.13	1.00	1.35
210a	0.0034	297.43	1.16	8.15	110.74	2.55	22.75	2.53	1.00	1.33
210b	0.0032	70.24	1.16	9.12	97.95	3.31	28.98	2.64	1.00	1.35
210c	0.0028	88.45	1.16	8.64	96.95	4.33	26.79	2.56	1.00	1.32

Table 12. Image analysis results of hoop Specimen 3 (240–330 degrees).

	Void Volume Fraction	Pore Area			Nearest Neighbor Distance			Aspect Ratio		
		Max. (µm)	Min. (µm)	Avg. (µm)	Max. (µm)	Min. (µm)	Avg. (µm)	Max. (µm)	Min. (µm)	Avg. (µm)
240a	0.0016	126.32	1.16	5.17	92.16	4.36	30.32	2.69	1.00	1.36
240b	0.0022	147.42	1.16	6.06	96.24	2.43	26.94	3.58	1.00	1.40
240c	0.0021	40.18	1.16	5.64	82.87	2.40	25.23	4.03	1.00	1.36
270a	0.0025	118.80	1.16	7.54	88.59	2.31	30.65	2.93	1.00	1.32
270b	0.0019	70.24	1.16	5.17	89.27	6.15	26.50	2.39	1.00	1.32
270c	0.0022	53.76	1.16	5.02	80.94	2.19	23.72	7.22	1.00	1.43
300a	0.0010	100.30	1.16	14.55	179.71	15.71	62.28	2.24	1.00	1.38
300b	0.0027	322.87	1.16	10.91	153.68	6.53	33.79	4.15	1.00	1.49
300c	0.0014	28.91	1.16	4.53	72.00	3.60	28.08	2.65	1.00	1.33
330a	0.0009	18.79	1.16	4.76	101.92	1.89	29.10	2.61	1.00	1.36
330b	0.0021	51.16	1.16	5.53	93.03	2.69	23.82	4.21	1.00	1.40
330c	0.0027	127.47	1.16	6.10	74.72	2.81	23.21	2.04	1.00	1.29

4 Summary

ERDC's Geotechnical and Structures Laboratory conducted laboratory experiments to characterize the mechanical properties and microstructure characteristics of steel cylindrical shells. To obtain the tensile stress-strain material responses, uniaxial tensile experiments were performed on ASTM dog-bone specimens and hoop cross-sectional specimens at displacement rates of 0.1 in./min. In addition to the mechanical property tests, the microstructure of the steel hoop cross-sections specimens was analyzed using a commercially available image-analysis software program to determine the VVF, NND of pores, maximum and minimum pore sizes, and aspect ratio of the pores. The results of the investigation allow for an understanding of the mechanical behavior of steel cylindrical shells.

The relationships between microstructure and the mechanical properties of the steel cylindrical shells were analyzed to obtain parameters that will be used as part of a geostatistical techniques project to model the cross-sectional porosity for mechanical analysis of crack initiation, growth, propagation, and coalescence when subjected to impulsive internal loads.

Reference

Stone, T. Y., L. Tucker, Y. Hammi, T. N. Williams, H. El Kadiri, and M. F. Horstemeyer. 2009. *Comparison of density measurement techniques for large PM components*. Journal of Powder Metallurgy, Under Review.

REPORT DOCUMENTATION PAGE

Form Approved
OMB No. 0704-0188

1. REPORT DATE *(DD-MM-YYYY)*	2. REPORT TYPE	3. DATES COVERED *(From - To)*
March 2012	Final	

4. TITLE AND SUBTITLE

Structure-Property Relationships of Steel Cylindrical Shells

5a. CONTRACT NUMBER

5b. GRANT NUMBER

5c. PROGRAM ELEMENT NUMBER

6. AUTHOR(S)

Ruth G. Hidalgo-Hernandez, Paul G. Allison, Brett A. Williams,
Luis A. de Béjar, W. Scott Hart, and Jason Morson

5d. PROJECT NUMBER

5e. TASK NUMBER

5f. WORK UNIT NUMBER

7. PERFORMING ORGANIZATION NAME(S) AND ADDRESS(ES)

Geotechnical and Structures Laboratory
U.S. Army Engineer Research and Development Center
3909 Halls Ferry Road
Vicksburg, MS 39180-6199

8. PERFORMING ORGANIZATION REPORT NUMBER

ERDC/GSL TR 12-13

9. SPONSORING / MONITORING AGENCY NAME(S) AND ADDRESS(ES)

U.S. Army Corps of Engineers

10. SPONSOR/MONITOR'S ACRONYM(S)

USACE

11. SPONSOR/MONITOR'S REPORT NUMBER(S)

12. DISTRIBUTION / AVAILABILITY STATEMENT

Approved for public release; distribution is unlimited.

13. SUPPLEMENTARY NOTES

14. ABSTRACT

Personnel of the U.S. Army Engineer Research and Development Center (ERDC), Geotechnical and Structures Laboratory (GSL), Engineering Systems and Materials Division (ESMD), Concrete and Materials Branch (CMB), Vicksburg, Mississippi, were asked to examine the mechanical properties and microstructure characteristics of a commercially available steel cylindrical shell in its as-manufactured condition. To examine the mechanical properties, uniaxial tensile experiments were performed on ASTM dog-bone specimens and hoop cross-sectional specimens at displacement rates of 0.1 in./min., to obtain the stress-strain material responses. A commercially available image-analysis program determined the void volume fraction (VVF), the nearest neighbor distance (NND) of pores, maximum and minimum pore sizes, and aspect ratio of the pores at 30-degree increments of the steel hoop cross-sections. The results of the investigation allow for an improved understanding of the mechanical behavior of steel cylindrical shells.

15. SUBJECT TERMS

Failure analysis
Cylindrical shells
Tensile experiments
Structure properties
Steel

16. SECURITY CLASSIFICATION OF:			17. LIMITATION OF ABSTRACT	18. NUMBER OF PAGES	19a. NAME OF RESPONSIBLE PERSON
a. REPORT	b. ABSTRACT	c. THIS PAGE			19b. TELEPHONE NUMBER *(include area code)*
Unclassified	Unclassified	Unclassified		20	